

Analyst

Accepted Manuscript



This is an *Accepted Manuscript*, which has been through the Royal Society of Chemistry peer review process and has been accepted for publication.

Accepted Manuscripts are published online shortly after acceptance, before technical editing, formatting and proof reading. Using this free service, authors can make their results available to the community, in citable form, before we publish the edited article. We will replace this *Accepted Manuscript* with the edited and formatted *Advance Article* as soon as it is available.

You can find more information about *Accepted Manuscripts* in the [Information for Authors](#).

Please note that technical editing may introduce minor changes to the text and/or graphics, which may alter content. The journal's standard [Terms & Conditions](#) and the [Ethical guidelines](#) still apply. In no event shall the Royal Society of Chemistry be held responsible for any errors or omissions in this *Accepted Manuscript* or any consequences arising from the use of any information it contains.

Cite this: DOI: 10.1039/c0xx00000x

www.rsc.org/xxxxxx

PAPER

Paper electrode integrated lateral flow immunosensor for quantitative analysis of oxidative stress induced DNA damage

Xuena Zhu¹, Pratikkumar Shah¹, Susan Stoff¹, Hongyun Liu² and Chen-zhong Li^{1*}*Received (in XXX, XXX) Xth XXXXXXXXXX 20XX, Accepted Xth XXXXXXXXXX 20XX*

DOI: 10.1039/b000000x

A novel device combining electrochemical and colorimetric detection is developed for the rapid measurement of 8-hydroxy-2'-deoxyguanosine (8-OHdG), a DNA oxidative damage biomarker. The device takes advantage of the speed and low cost of the conventional strip test as well as the high reliability and accuracy of electrochemical assay. Competitive immunoreactions were performed on the lateral flow strip, and the captured 8-OHdG on the control line was determined by chronoamperometric measurement with carbon nanotubes paper as the working electrode. At the same time, the color intensity of the test line was measured by a scanner and analyzed by the ImageJ software. The device was able to detect 8-OHdG concentrations in PBS as low as 2.07 ng mL⁻¹ by the colorimetric method and 3.11 ng mL⁻¹ by the electrochemical method. Furthermore, the device was successfully utilized to detect 8-OHdG in urine with a detection limit of 5.76 ng mL⁻¹ (colorimetric method) and 8.85 ng mL⁻¹ (electrochemical method), respectively. In conclusion, the integrated device with dual detections can provide a rapid, visual, quantitative and feasible detection method for 8-OHdG. The integration of these two methods holds two major advantages over tests based on single method. Firstly, it can provide double confidence on the same assay. Secondly, by involving two methods that differ in principle, the integration could potentially avoid false results coming from one method. In addition, these methods do not require expensive equipment or trained personnel, deeming it suitable for use as a simple, economical, portable field kit for on-site monitoring of 8-OHdG in a variety of clinical settings.

Introduction

In living cells endogenous reactive oxygen species (ROS) are produced as a result of various physiological processes, metabolic and other biochemical reactions. ROS, at low concentrations can serve as signaling molecules, necessary for the normal cellular activities. However, an increase in the level of ROS from exogenous sources such as ultraviolet or ionizing radiation, cigarette smoking, hazardous chemicals, etc.¹ can lead to an abnormal oxidant system, called oxidative stress.² In the presence of oxidative stress, lipids, proteins and nucleic acids present in the cell may undergo oxidative damage. This damage, if unrepaired, accumulates and leads to physiological attrition and an increased risk of several chronic diseases, such as cancer, diabetes, cardiovascular disease, and neurodegenerative diseases.³

Numerous DNA damage products are formed during ROS induced oxidation. Among the four constituent bases of DNA, guanine in particular is the most readily oxidized. Upon oxidation, a hydroxyl group is added to the C-8 position of deoxyguanosine in DNA,⁴ resulting in the production of 8-hydroxy-2-deoxyguanosine (8-OHdG), one of the predominant forms of free radical-induced lesions of DNA and the most commonly studied biomarker for assessing oxidative stress.^{5, 6} Following the damage, cells have the capability to recognize and

remove the oxidative lesion by the base excision repair mechanism (BER). During repair, the oxidized guanine is cleaved by enzymes such as endonuclease and glycosylase,^{7, 8} secreted out of the cell into the blood and excreted via the urine.^{9, 10} Thus, the urinary excretion of 8-OHdG reflects oxidative DNA damage and the "whole body" repair capacity.¹¹ Rapid monitoring of 8-OHdG following suspected exposure to dangerous agents is critical to identifying pre-symptomatic states, high risk situations, and early stages of illness. Levels of 8-OHdG are expected to be proportional to the duration of exposure and the exposure level.

The most commonly used analytical techniques for the detection of 8-OHdG are high-performance liquid chromatography-Electrochemical detection (HPLC-ECD),^{12, 13} HPLC tandem mass spectrometry,^{14, 15} gas chromatography-mass spectrometry (GC-MS),¹⁶ Capillary electrophoresis with electrochemical detection (CE-ECD)¹⁷ and Enzyme-linked Immunosorbent Assay (ELISA).^{18, 19} These methods have been successfully used to analyze 8-OHdG in cell lysates, fluid samples and organs. However, these are lab based techniques requiring costly and cumbersome equipment and trained personal to perform the measurements. Thus, these techniques are of limited use in close proximity to patients. There is a great need for a portable, point-of-care-testing (POCT) device for use by the mass public for easily available biological samples such as urine, saliva, blood, etc.³² An ideal POCT device would serve the

purpose of rapid and accurate detection of 8-OHdG with a user friendly operation eliminating the need for lab facilities and professionals.³⁰ This POCT device would provide results in minutes rather than days or weeks and eliminate the concerns involved with the transport and storage of biological samples.

Lateral flow immunochromatographic assay, also known as Immunochromatographic test strip, can provide a low-cost, easy-to-use and portable platform and have been widely used in many areas.^{20-24,31} In a lateral flow strip, the primary goal is to visualize colorimetrically the qualitative or semi-quantitative status of the analytes. Readout of the test results is performed optically, either by a machine such as a reflectometer or by the unaided human eye. In our previous studies, we have successfully detected 8-OHdG both in pure solution and cell lysates using the lab-developed gold nanoparticles (AuNPs) based lateral-flow immunostrip.²⁵ However, lateral flow immunostrip is known more prone to develop false positive or false negative result if applied to real samples, such as urine and blood, especially patient originated ones. The absorption of antibodies on the surface of AuNPs heavily relies on the hydrophobic and ionic interaction. A “bad” sample with either high ionic strength, high urea concentration or low pH²⁶ accelerates the dissociation of the antibody-AuNPs complex, leading to false results.

Electrochemical detection is an attractive method due to its capability of quantitative analysis, easy to be miniaturized to be a portable formation, and less incident background. 8-OHdG undergoes oxidation via a two-electron two-proton charge transfer reaction.²⁷ This electrochemistry property has been well characterized for quantitative measurement.²⁸ The only concern with the measurement of 8-OHdG by electrochemical method is the potential interference of 8-OHdG containing short nucleotides. As the products of 8-OHdG repairing, both 8-OHdG molecule and 8-OHdG containing short nucleotides present in biological urine samples, with 8-OHdG as the major form usually. Existence of 8-OHdG containing short nucleotides will significantly quench the signaling in electrochemical assay set up with parameters for 8-OHdG molecule. The occurrence and proportion of 8-OHdG containing short nucleotide is relatively similar in normal biological samples, but might vary appreciably across normal person and patients.

To overcome the drawbacks of immunostrip assay and electrochemical method for 8-OHdG detection, we design and report here a novel sensing system by integrating carbon nanotubes (CNTs) paper electrodes and immunochromatographic strip (referred to as an electrochemical immunosensor, ECIS) for quantitative analysis of 8-OHdG in both standard solution and urine samples. The sensing device combined competitive AuNPs based immunoassay of lateral-flow format with miniaturized paper electrodes for both colorimetric and electrochemical detection. On one hand, electrochemistry does not rely on the conjugation of AuNPs and antibody, and thus could function normally when the colorimetric method gives false positive results due to dissociation of AuNPs from antibody. On the other hand, immunostrip assay is able to respond to both 8-OHdG molecule and 8-OHdG containing short nucleotides and thus functions normally for biological samples containing abnormally high 8-OHdG containing short nucleotides. The optimized system was capable of achieving a detection limit of 2.07 ng mL⁻¹ for 8-

OHDG while only requiring 10 min to complete the assay. This novel test strip will provide a useful method for quantitative assessment of DNA oxidative stress with high sensitivity, specificity, speed of detection and the advantage of minimized false results. Further more, the integrated platform can be further upgraded and optimized into a wireless-enabled biosensing system in future.

Materials and methods

Materials and Equipments

Nitrocellulose membrane, glass fibers, absorbent materials and polyester backing materials were acquired from Millipore (Billerica, MA). Buckeye CNT paper was purchased from Buckeye Composites NanoTechLabs, Inc. (Kettering, OH). Silver/Silver Chloride conductive ink was obtained from Conductive Compounds, Inc. (Hudson, NH). Mouse monoclonal antibodies to 8-hydroxyguanosine and polyclonal Goat anti Mouse IgG were purchased from Abcam (Cambridge, MA). 8-hydroxy Guanosine and 8-hydroxy-2-deoxy Guanosine were purchased from Cayman chemical (Ann Arbor, MI). Gold chloride trihydrate (HAuCl₄ · 3H₂O), Sodium periodate (NaIO₄), Sodium phosphate (Na₃PO₄), Sodium chloride (NaCl), Sodium borohydride (NaBH₄), Potassium carbonate (K₂CO₃), Ethylene Glycol and Bovine serum albumin (powder) were purchased from Sigma-Aldrich (St. Louis, MO). Silver conductive adhesive paste, Tri-Sodium Citrate Dihydrate, Triton X-100 and Phosphate buffered saline (PBS, 1X, PH=7.4) were purchased from VWR (West Chester, PA). Tris-HCl (1 M), Tween® 20 (polyoxyethylene-20-sorbitan monolaurate) and Sucrose were purchased from Fisher Scientific (Fairlawn, NJ). The Zetasizer was purchased from Malvern Instruments, (Woodstock, GA). The Laminator was purchased from Office Depot. HP Scanjet G3110 Photo Scanner was bought from Hewlett-Packard (Palo Alto, CA). Dispenser Linomat 5 was purchased from CAMAG (Wilmington, NC). Drying Oven was purchased from VWR (West Chester, PA). Cyclic voltammetric (CV) and Chronoamperometric measurements were performed with an electrochemical analyzer CHI 660C (CH Instruments, Austin, TX). ImageJ and SigmaPlot software were downloaded from the internet.

Preparation of immunochromatographic strip

The lateral flow immunostrip specific for 8-OHdG detection was prepared following the similar method established by our lab²⁵ with slight modification. Briefly, the immunostrip consists of four components: sample loading pad, conjugated pad, nitrocellulose membrane, and absorption pad, all of which were pasted onto a plastic backing plate. AuNPs with average diameter 20 nm were synthesized by a modified citrate reduction method.²⁹ Ab-AuNPs conjugates and BSA-8 hydroxyguanosine conjugates were prepared according to the reported protocol.²⁵ A desired volume (25 μL) of Ab-AuNPs mixture was dispensed by pipette onto a glass fiber pad (6 mm × 5 mm), which was dried at room temperature and stored in desiccators at 4 °C before use. The sample loading pad (6 mm × 16 mm) was made from glass fiber and soaked with a buffer containing 0.15 mM NaCl, 0.05 M Tris-HCl and 0.25% Triton X-100. The pad was dried in an oven for 20 min at 50 °C and stored in desiccators at room temperature.

BSA-8 hydroxyguanosine conjugates were used as the test line (T) capture reagent, while goat anti-mouse IgG (1 mg mL^{-1}) was used as the control line (C) capture reagent. These capture reagents were dispensed by the Linomat 5 dispenser at different locations on a nitrocellulose membrane ($30 \text{ mm} \times 10 \text{ cm}$) as the test and control lines (separation distance is 13 mm). The membrane had been mounted onto the adhesive backing plate in advance. The prepared plate (with nitrocellulose membrane and absorption pad) was cut into 6 mm-wide strips using a strip cutter and stored at $4 \text{ }^\circ\text{C}$ until use. Finally, all of other parts were assembled on the adhesive backing layer. Each part overlapped 2 mm to ensure the solution migration through the strip during the assay.

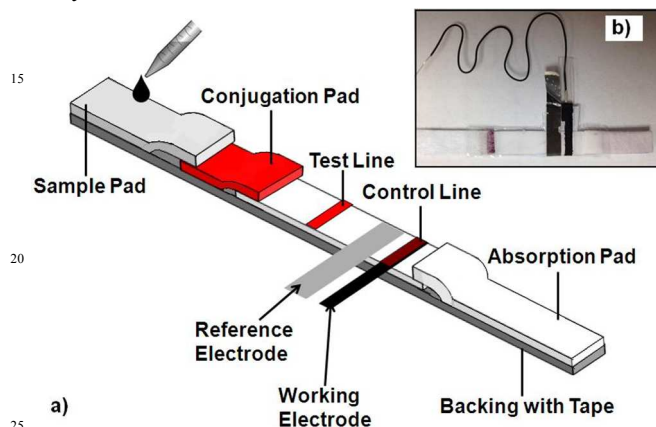


Fig. 1 (a) A schematic for ECIS; (b) Photograph of a representative ECIS.

Fabrication of CNTs conductive paper integrated immunostrip (ECIS)

The structure of ECIS (Fig. 1) is similar to that of the traditional lateral flow test strip discussed in the previous section. Besides the four required components, two electrodes were integrated into the original strip to carry out the electrochemical detection function. Briefly, CNTs conductive paper (2 mm in width) bought from Buckeye Composites was used as the working electrode. The CNTs paper was placed on the control line with the sensing surface facing down, and its extension beyond the strip was laminated with a silver plated copper wire to be connected to an electrochemical analyzer. Ag/AgCl ink painted copper paper (4 mm in width) was placed at a 1 mm distance from the CNTs paper on the side farthest from the absorption pad to serve as the reference/counter electrode. Finally, the entire strip was laminated (Fig. 1 (b)) in order to ensure complete contact between the sample, membrane and electrodes.

Preparation of standards solutions and spiked urine samples

A stock solution of 8-OHdG ($500 \text{ } \mu\text{g mL}^{-1}$) was prepared by dissolving 8-OHdG powder in purified PBS (1X) solution and kept at $4 \text{ }^\circ\text{C}$. Working standards ($(1-1000) \text{ ng mL}^{-1}$) were prepared with the same buffer before each use.

Bland urine samples were obtained from drug free healthy volunteers within the department following the protocol approved by both Florida International University (FIU) and the Telemedicine and Advanced Technology Research Center [TATRC] institutional review boards (IRB). Samples were filtered through a Whatman no. 1 filter paper, and stored frozen ($-20 \text{ }^\circ\text{C}$) in aliquots of 4 mL until analyzed. Before use, urine samples were thawed to room temperature and then centrifuged at

$7,000 \text{ rcf}$ for 10 min to remove any precipitate. After which, the supernatants were collected and diluted 10 fold with PBS (1X) to minimized the interference induced by variation of urine components. The diluted urine samples were serially spiked with 8-OHdG to make solutions of 0, 1, 10, 20, 50, 80, 100, 150, 200 and 1000 ng mL^{-1} concentration levels prior to the test.

Coupled chronoamperometric and colorimetric measurements of 8-OHdG

Chronoamperometric measurements were performed with an electrochemical analyzer CHI 660C or a portable electrochemical analyzer connected to a personal computer. A fully-integrated ECIS sensor was connected to the analyzer in advance and conductivity of the loop was examined. $100 \text{ } \mu\text{L}$ of standard solution or of urine sample solution containing the desired concentration of 8-OHdG was applied to the sample application zone. After waiting for a specified time period (10 min), chronoamperimetric measurements (fixed potential: 0.42 V , sample duration: 20s) were performed by using the software. At the same time, a photograph of the strip was then taken using a digital scanner. The software ImageJ was used to quantify the intensity of test lines for colorimetric analysis.

Quantitative analysis

Current readout from chronoamperimetric measurements and color intensity from colorimetric tests are expressed as the mean \pm SD of three experiments. The data were analyzed quantitatively either by using ImageJ and/or Excel software.

Results and discussion

Material selection for electrochemical sensing system-CNTs paper

Suitable materials of electrode need to be selected for the electrochemical sensing system. We fabricated several screen-printed electrodes by using different electrode materials and different substrates, such as silver-based electrodes and gold thin-film electrodes. We also tried various commercialized screen-printed electrodes which are constructed by more advanced nanomaterials including graphene electrodes, gold nanoparticle decorated electrodes and CNTs electrodes. These electrodes have their own advantages and disadvantages in terms of sensitivity, simplicity and cost-effectiveness. However, based on their performances on 8-OHdG detection and the design of the sensor, a flexible electrode which can be easily integrated into the strip and of high electrochemical activity is preferred. CNTs conductive paper, bought from NanoTechLabs, Inc., was finally selected as the electrochemical sensing component as it is flexible as well as has high electrochemical activity. Before using the CNTs conductive paper to create the test strip, we characterized the CNTs paper by using scanning electron microscope (SEM). The surface structure of CNTs conductive paper is shown in Fig. 2. Instead of the sheet or net structure most often found in CNTs, the figure shows a forest structure which can provide a larger surface area and better sensitivity, both qualities which are suitable for our applications.

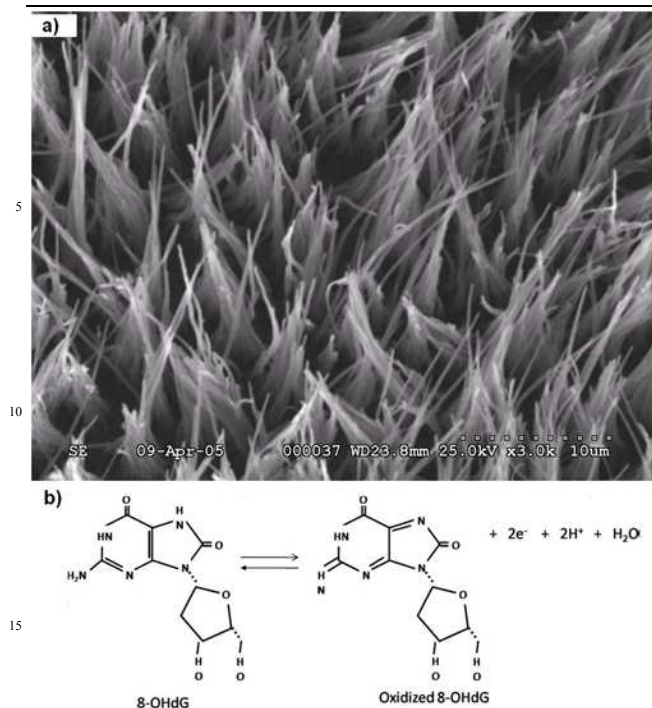


Fig. 2 (a) SEM characterization of CNTs paper; (b) Schematic showing the electroactive behavior of 8-OHdG.

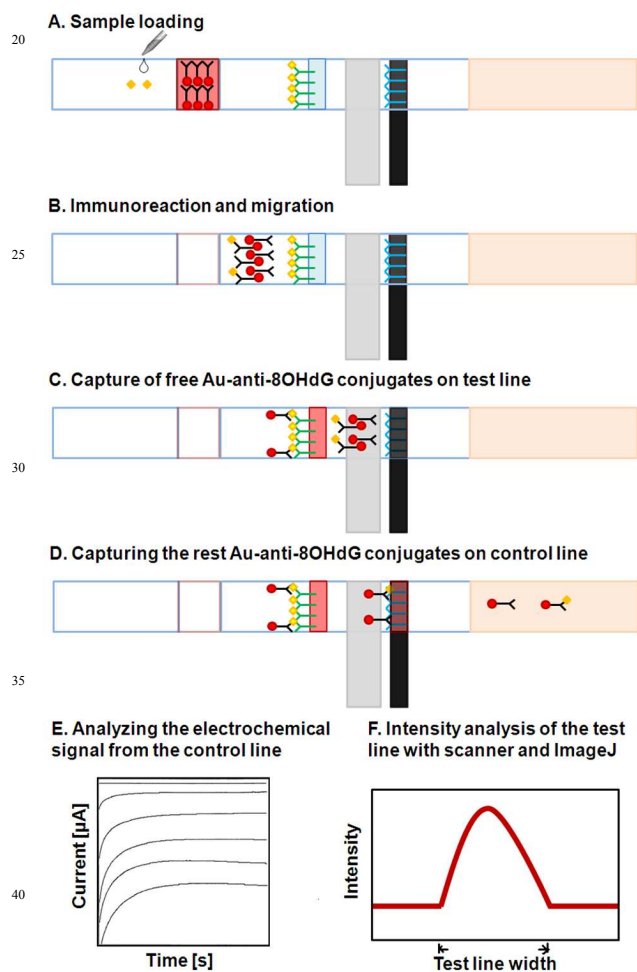


Fig. 3 Principle of the ECIS for 8-OHdG quantitative detection.

Principle of the ECIS for 8-OHdG detection

The method of the biosensor is based on two principles: the first principle is that of competitive-type immunoreactions in the lateral flow strip as demonstrated in our previous publication,²⁵ the second principle is the ability of 8-OHdG to be electrochemically detected when undergoing oxidation via a two-electron two-proton charge transfer reaction, shown in Fig. 2 (b).²⁷

In a typical assay, a sample solution containing a desired concentration of 8-OHdG is applied to the sample application pad (Fig. 3 (A)). The sample moves along the strip due to capillary force and rehydrates the AuNP-anti-8-OHdG in the conjugation pad. Then the immunoreactions between 8-OHdG and AuNP-anti-8-OHdG conjugates occur and the formed AuNP-anti-8-OHdG-8-OHdG complexes continue to migrate along the strip (Fig. 3 (B)). When they reach the test zone, the unbound AuNP-anti-8-OHdG conjugates are captured by the BSA-8-hydroxyguanosine conjugates immobilized on the test zone via the same immunoreactions. The accumulation of AuNPs on the test zone induces a characteristic red band which is visible with the naked eye (Fig. 3 (C)). This color change accomplishes the colorimetric detection of 8-OHdG in a sample and the color intensity is inversely proportional to the concentration. The capillary action causes the liquid sample to migrate further. Once the solution passes through the control zone, the AuNP-anti-8-OHdG Ab-8-OHdG complexes and excess AuNP-anti-8-OHdG conjugates are captured on the control zone by the pre-immobilized polyclonal Goat anti-Mouse IgG, thus forming a second red band showing that the biosensor is operating properly (Fig. 3 (D)). Chronoamperometric measurement of the control line was performed (at exact 10 min after applying the sample) using electrochemical analyzer providing the data to produce the Current vs. Time curves (Fig. 3 (E)). Qualitative analysis of the colorimetric test is simply performed by observing the color change of the test zone, and quantitative analysis is realized by reading the optical intensities of the red bands with a scanner (just after the chronoamperometric measurement). The peak area (Fig. 3 (F)) is proportional to the amount of the captured Au-NPs in the test zone, which is inversely proportional to the concentration of 8-OHdG in the sample solution.

Electrochemical characterization of CNTs conductive paper-based electrode

Before using ECIS devices for analytes measurement, the functionality of the electrodes was established. A potassium ferricyanide/ferrocyanide ($K_3Fe(CN)_6/K_4Fe(CN)_6$) mixture was used as a model redox-active compound to characterize electrochemical behavior of the CNTs conductive paper. 100 mM $K_3Fe(CN)_6/K_4Fe(CN)_6$ stock solution was prepared by dissolving these two chemicals in PBS (1X) buffer, corresponding working solutions can be obtained by altering the dilution. Fig. 4 shows the cyclic voltammetric response for the compound in the two electrode system at various scan rates. The peak shape of CVs demonstrates a typical reversible electrochemical reaction, indicating that no side reactions take place and the kinetics of electron transfer is sufficiently rapid to maintain the surface concentrations of redox-active species at the values required by the Nernst equation. Next, the dependence of peak current on the

square root of the scan rate was studied. The insert in Fig. 4 shows that anodic and cathodic peak currents were directly proportional to the square root of the scan rate ($v^{1/2}$) between 10 and 200 mV s^{-1} . The linearity indicates that the mass transfer in this system is a diffusion controlled process similar to the behavior of traditional electrochemical cells.

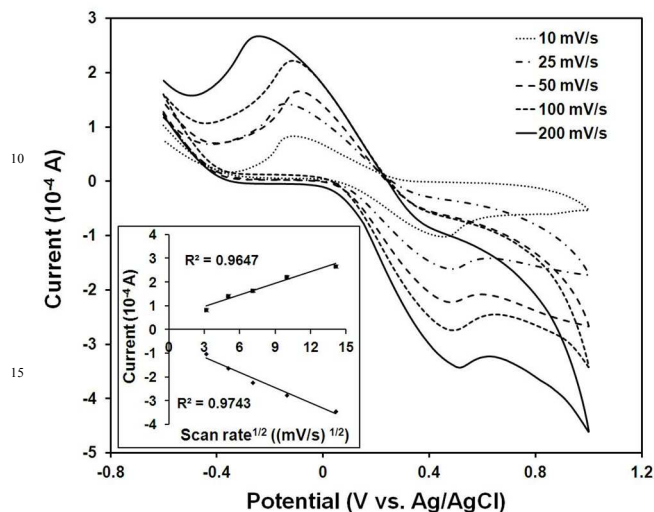


Fig. 4 Representative cyclic voltammograms of 5.0 mM $\text{K}_3\text{Fe}(\text{CN})_6/\text{K}_4\text{Fe}(\text{CN})_6$ solution ($\text{pH}=7.0$) in two electrodes system at various scan rates: 10, 25, 50, 100, and 200 mV s^{-1} . We used a 2 mm by 6 mm CNT conductive paper electrode as the working electrode, and a printed Ag/AgCl electrode as the reference/counter electrode. The relationship between anodic and cathodic currents and the square root of the scan rate is shown in the insert. The red lines represent the linear regression line between $i_{p,ox}$ or $i_{p,re}$ and $(v)^{1/2}$, respectively.

Colorimetric measurement of analytes in buffer by ECIS

A series of 8-OHdG standard solutions with concentrations of 0, 1, 10, 20, 50, 80, 100, 150, 200, and 1000 ng mL^{-1} in 1X PBS buffer were prepared and applied to the strips. After 10 min, chronoamperometry at the electrodes and color intensity of the test lines were recorded according to the method in the methodology section. The color bar (Fig. 5 (a)) shows the typical responses on test lines of the strips to 8-OHdG with increasing concentrations from 0 to 1000 ng mL^{-1} . The color intensity decreased when the sample concentration increased which is consistent with the theory of competitive format detection. The color bar can easily be used as a reference, each color representative of the results for equivalent concentration of the analyte.

Fig. 5 (b) demonstrates the calibration curve produced by introducing samples of varying concentrations of 8-OHdG into the strips, revealing a logarithmic relationship between the color intensity and the concentration. Normalized intensity defined by ASD (average sample density) / ABD (average blank density) of the test line is used as the y-axis. As these are intended to be single-use test strips, each data point represents the average response from three separate test strips. The error bars represent the standard deviation. Most commercialized ELISA kit can detect urinary 8-OHdG concentration in the range of 0.64 to 200 ng mL^{-1} (i.e. KOG-200SE, Genox). This range was used as a reference for linearity study. The insert for Fig. 5 (b) shows that a linear response is observed for the concentrations between 1 ng mL^{-1} and 200 ng mL^{-1} (logarithm scale) where the coefficient of

determination (R^2) is greater than 0.99. The limit of detection (LOD), calculated based on three times the standard deviation of blank, was found to be 2.07 ng mL^{-1} . The result shows that this strip can potentially be used as a simple, rapid (~10 min) and low cost (\$) platform for 8-OHdG measurement.

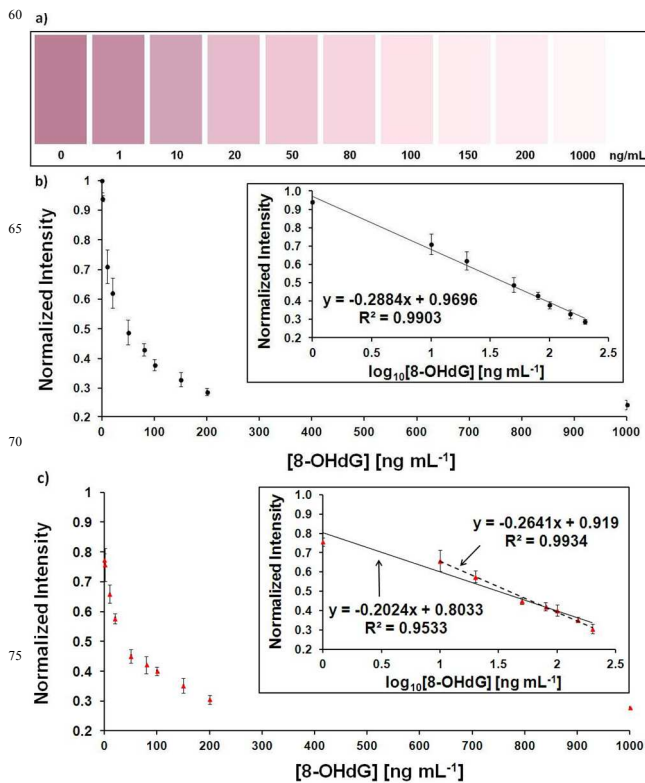


Fig. 5 (a) Color bar represents 8-OHdG standard solutions with varying concentrations. (b) Dose-response curve for 8-OHdG based on optical density analysis using standard samples. Values are mean SD from three independent experiments. The normalized intensity of the test line is plotted against the concentration of 8-OHdG in the logarithm scale as shown in the insert. (c) Dose-response curve for 8-OHdG based on optical density analysis using urine samples. Values are mean SD from three independent experiments. The normalized intensity of the test line is plotted against the concentration of 8-OHdG in the logarithm scale as shown in the insert (solid line, 1-200 ng mL^{-1} ; dash line, 10-200 ng mL^{-1}).

Colorimetric measurement of analytes in urine samples by ECIS

After confirming the feasibility of this strip for standard 8-OHdG solutions measurement, it was evaluated as a tool for urine sample testing. A series of 8-OHdG spiked urine samples with the same concentrations of those in PBS buffer were prepared and applied to the strips.

Fig. 5 (c) shows the normalized intensity curve rendered from the urine samples spiked with varying 8-OHdG concentrations. As expected, the changing trend of the curve is similar to that of the standard solutions. We also drew two linear fitting curves for the urine samples over the whole and partial concentration range (solid line, 1-200 ng mL^{-1} ; dash line, 10-200 ng mL^{-1}), shown in the insert. A linear response is also observed for the concentration between 1 ng mL^{-1} and 200 ng mL^{-1} (logarithm scale) where the coefficient of determination (R^2) is greater than 0.95. The LOD, calculated as previous method, was found to be 5.76 ng mL^{-1} , which is still low enough for 8-OHdG

measurement in urine samples from both healthy and non-healthy patients (Typically, healthy human subjects have urinary 8-OHdG levels in the range of 20 to 80 ng mL⁻¹. While the levels will go up 2~3 times higher for the non-healthy patients depend on 5 different types of diseases).

The slope obtained from the whole range fitting (solid line) is significantly bigger than that generated from spiked PBS samples. This should majorly be caused by the originally present 8-OHdG in human urine (2-8 ng mL⁻¹ after 1/10 dilution) that introduce a 10 considerable concentration shift for the left end data. For this reason the dash line produce a more accurate fitting with R² as high as 0.9934 and slope of -0.2641 which is much closer to that of spiked PBS sample.

Nevertheless, in reality there are various types of bio- 15 molecules in the real urine which can affect the antigen-antibody interaction and stability of antibody-AuNP complex, leading to lower discrimination among different 8-OHdG concentrations. This presents the major reason why we still get a bigger slope in spiked urine samples even after the deletion of first data point 20 when compared to that of PBS. It is worth note that, as a universal issue for immunoassays, biological samples from different individuals may interfere with immuno-reactions differentially. There are some easy methods that could be used, such as 1/10 dilution for personal testing and molecular size 25 based filtration or centrifugation in laboratory, to minimize these difference in interference. A complete establishment of a marketed immunoassay for a particular molecule still requires the evaluation of different interference of samples from individuals across normal person and patients, which is one of our follow-ups 30 in future works.

Chronoamperometric analysis of 8-OHdG in the ECIS

At the start of our study, we employed numerous electrochemical techniques including cyclic voltammetry, square wave voltammetry, etc for 8-OHdG measurement in the ECIS system. 35 For most techniques, 8-OHdG can only be detected in high

concentrations, making such techniques unsuitable for use in clinical research. Chronoamperometry, which offers a better signal-to-noise ratio than other electrochemical techniques, is able to detect 8-OHdG in lower concentrations. Thus, this method 40 was used as the standard detection approach for the following study.

Prior to chronoamperometric measurement, cyclic voltammetry was used to determine the oxidation potential of 8-OHdG (0.42 V) in the ECIS system with high concentration. 45 Subsequently, chronoamperometric measurements were performed at fixed step potential (0.42 V) after applying the 8-OHdG samples (standard or urine) to the strips for 10 min (just before taking the photographs for colorimetric tests). Fig. 6 (a) shows a representative chronoamperometric response to the 50 measurements of 8-OHdG using ECIS. Over the range of concentrations of 8-OHdG examined (0–150 ng mL⁻¹), all the response curves reached a steady state 2 s after the step potential. Fig. 6 (b) shows the corresponding calibration curves for the detection of 8-OHdG in both standard and urine solutions. When 55 the concentration of 8-OHdG is in the range of 0-150 ng mL⁻¹, the current is linearly proportional to the 8-OHdG concentration with the correlation coefficient of R² = 0.99 in standard solutions and that of R² = 0.97 in urine samples. From the calibration plot, comparable detection limits (compared to the 60 colorimetric method) of 3.11 ng mL⁻¹ in standard solutions and 8.85 ng mL⁻¹ in urine samples were calculated, which are still sensitive enough for 8-OHdG measurement in human urine samples.

Both the higher detection limitation and bigger slope in spiked 65 urine samples indicate that background of urine lower the sensitivity of electrochemical detection of 8-OHdG indicated by the difference in slopes. This is as expected because biological urine definitely has a completely different ionic environment where electrochemistry will occur quantitatively 70 differently.

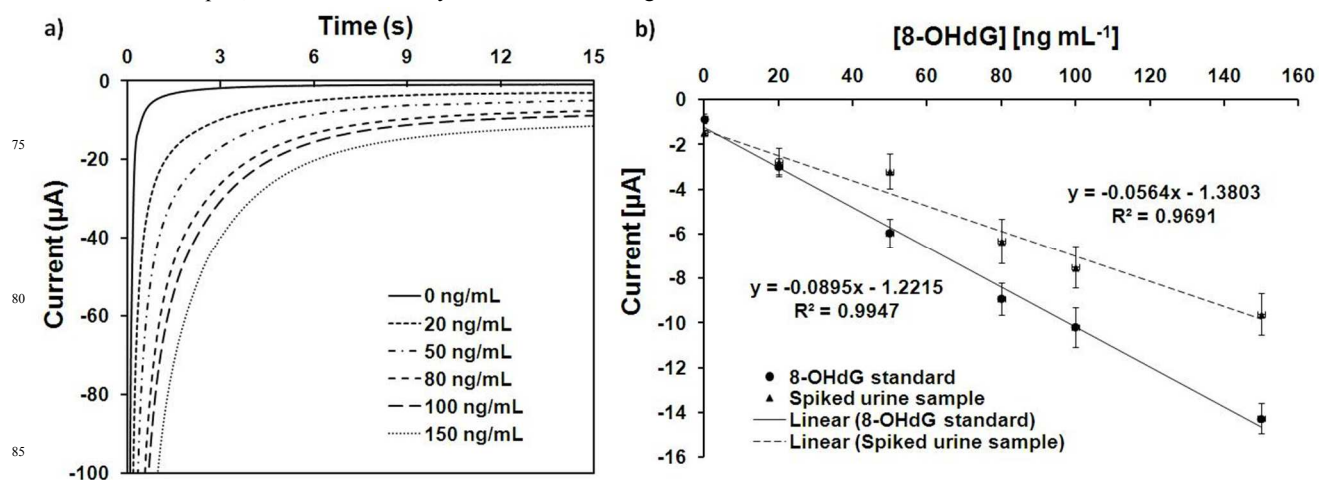


Fig. 6 (a) Representative chronoamperometric curves for 8-OHdG concentrations (ng mL⁻¹): 0, 20, 50, 80, 100 and 150 in the ECIS; (b) Calibration plots of current as a function of the 8-OHdG concentration for its detection in standard solutions (black circle) and in urine samples (black triangle). We used CNTs conductive paper as the working electrode and silver/silver chloride as the counter/reference electrode, respectively. The working electrode had a surface area of 12 mm² in contact with the solution in both standard and urine. The distance between electrodes was 1.0 mm. A 420 mV step potential was used to generate the calibration curve. The solid lines represent a linear fit to standard with regression equation: $y = -1.2215 - 0.0895x$ ($R^2 = 0.9947$, $n=3$). The dash line represents a linear fit to urine samples with the regression equation: $y = -1.3803 - 0.0564x$ ($R^2 = 0.9691$, $n=3$).

Conclusions

We demonstrate, for the first time, the coupling of CNTs conductive paper based electrochemical detection and traditional lateral flow immunostrip based colorimetric detection to provide rapid (~10 min) quantitative measurement of DNA oxidative damage biomarkers (8-OHdG) in both PBS and spiked urine samples, exhibiting the feasibility of using this device in medical diagnosis. The two methods on one single strip are both able to quantitatively detect levels of 8-OHdG concentrations, with detection limitation of 2.07 ng mL⁻¹ for colorimetric method and 3.11 ng mL⁻¹ for electrochemical method that are low enough for patient testing in the field. Integration of these two detections provides a platform where cross check of 8-OHdG measurement could be achieved. On one hand, tester could get higher confidence on double positive or double negative results. On the other hand, this system minimizes the chance of false negative or false positive by compensation between these two methods differing in principle. Future effort will be made to optimize our system to be suitable to get connected to a wireless-enabled electronic system for portable and quantitative assessment of oxidative stress induced DNA damage.

Acknowledgements

This research and development project was supported by the grant NIH R15 ES021079-01 and the grant W81XWH-10-1-0732 by U.S. Army Medical Research & Materiel Command (USAMRMC) and the Telemedicine & Advanced Technology Research Center (TATRC).

Notes and references

¹Nanobioengineering/Bioelectronics Laboratory, Department of Biomedical Engineering, Florida International University, 10555 West Flagler Street, Miami, FL 33174, USA. Fax: (305) 348 6954; Tel: (305) 348 0120; E-mail: licz@fiu.edu

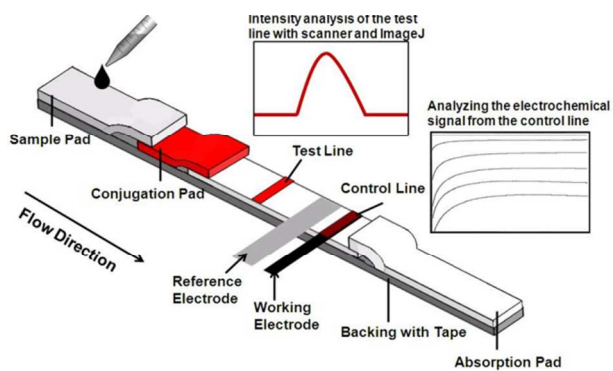
²Department of Chemistry, Beijing Normal University, Beijing 100875, China

* Prof. C.-Z. Li. Corresponding-Author, E-mail: licz@fiu.edu;

- 1 K. R. Martin and J. C. Barrett, *Hum Exp Toxicol*, 2002, **21**, 71-75.
- 2 B. Halliwell and J. M. C. Gutteridge, *Free Radicals in Biology and Medicine*, Oxford University Press, New York, 2007.
- 3 L. L. Wu, C. C. Chiou, P. Y. Chang and J. T. Wu, *Clin Chim Acta*, 2004, **339**, 1-9.
- 4 R. A. Floyd, J. J. Watson, P. K. Wong, D. H. Altmiller and R. C. Rickard, *Free Radic Res Commun*, 1986, **1**, 163-172.
- 5 H. Kasai, *Mutat Res-Rev Mutat*, 1997, **387**, 147-163.
- 6 M. K. Shigenaga, C. J. Gimeno and B. N. Ames, *Proc Natl Acad Sci U S A*, 1989, **86**, 9697-9701.
- 7 M. Hollstein, D. Sidransky, B. Vogelstein and C. C. Harris, *Science*, 1991, **253**, 49-53.
- 8 K. C. Cheng, D. S. Cahill, H. Kasai, S. Nishimura and L. A. Loeb, *J Biol Chem*, 1992, **267**, 166-172.
- 9 M. K. Shigenaga and B. N. Ames, *Free Radic Biol Med*, 1991, **10**, 211-216.
- 10 S. Loft, K. Vistisen, M. Ewertz, A. Tjonneland, K. Overvad and H. E. Poulsen, *Carcinogenesis*, 1992, **13**, 2241-2247.
- 11 O. I. Aruoma and B. Halliwell, *DNA and Free Radicals: Techniques, Mechanisms and Applications*, OICA International (UK) Limited, 1998.
- 12 S. Koide, Y. Kinoshita, N. Ito, J. Kimura, K. Yokoyama and I. Karube, *J Chromatogr B Analyt Technol Biomed Life Sci*, 2010, **878**, 2163-2167.
- 13 A. M. Domijan and M. Peraica, *Arh Hig Rada Toksikol*, 2008, **59**, 277-282.
- 14 M. Harri, H. Kasai, T. Mori, J. Tornaues, K. Savela and K. Peltonen, *J Chromatogr B Analyt Technol Biomed Life Sci*, 2007, **853**, 242-246.
- 15 A. Weimann, D. Belling and H. E. Poulsen, *Nucleic Acids Res*, 2002, **30**, E7.
- 16 H. S. Lin, A. M. Jenner, C. N. Ong, S. H. Huang, M. Whiteman and B. Halliwell, *Biochem J*, 2004, **380**, 541-548.
- 17 D. J. Weiss and C. E. Lunte, *Electrophoresis*, 2000, **21**, 2080-2085.
- 18 M. S. Cooke, R. Singh, G. K. Hall, V. Mistry, T. L. Duarte, P. B. Farmer and M. D. Evans, *Free Radic Biol Med*, 2006, **41**, 1829-1836.
- 19 R. Yoshida, Y. Ogawa and H. Kasai, *Cancer Epidemiol Biomarkers Prev*, 2002, **11**, 1076-1081.
- 20 G. Liu, X. Mao, J. A. Phillips, H. Xu, W. Tan and L. Zeng, *Anal Chem*, 2009, **81**, 10013-10018.
- 21 Q. Zeng, X. Mao, H. Xu, S. Wang and G. Liu, *Am. J. Biomed. Sci.*, 2009, **1**, 70-79.
- 22 L. Wang, W. Ma, W. Chen, L. Liu, Y. Zhu, L. Xu, H. Kuang and C. Xu, *Biosens Bioelectron*, 2011, **26**, 3059-3062.
- 23 F. Lu, K. H. Wang and Y. Lin, *Analyst*, 2005, **130**, 1513-1517.
- 24 W. Dungechai, O. Chailapakul and C. S. Henry, *Anal Chim Acta*, 2010, **674**, 227-233.
- 25 X. Zhu, E. Hondroulis, W. Liu and C. Z. Li, *Small*, 2013, **9**, 1821-1830.
- 26 M. Raoof, S. J. Corr, W. D. Kaluarachchi, K. L. Massey, K. Briggs, C. Zhu, M. A. Cheney, L. J. Wilson and S. A. Curley, *Nanomedicine*, 2012, **8**, 1096-1105.
- 27 R. N. Goyal, N. Jain and D. K. Garg, *Bioelectroch Bioener*, 1997, **43**, 105-114.
- 28 S. Prabhulkar and C. Z. Li, *Biosensors and Bioelectronics*, 2010, **26**, 1743-1749.
- 29 K. C. Grabar, R. G. Freeman, M. B. Hommer and M. J. Natan, *Anal Chem*, 1995, **67**, 735-743.
- 30 P. Shah, X. Zhu, C. Chen, Y. Hu, C.-Z. Li, *Biomedical Microdevices*, DOI 10.1007/s10544-013-9803-7, 2013.
- 31 C.-Z. Li, K. Vandenberg, S. Prabhulkar, X. Zhu, L. Schneper, K. Methee, C.J. Rosser, E. Almeida, *Biosensors and Bioelectronics*, 2011, **26**, 4342-4348.
- 32 E. Hondroulis, C.-Z. Li, Impedance based Nanotoxicity Assessment of Graphene Nanomaterials at Cellular and Tissue Level, *Analytical Letters*. 2011, **45**, 272-282.

1
2
3
4
5
6
7
8
9
10
11
12
13
14
15
16
17
18
19
20
21
22
23
24
25
26
27
28
29
30
31
32
33
34
35
36
37
38
39
40
41
42
43
44
45
46
47
48
49
50
51
52
53
54
55
56
57
58
59
60

For Table of contents entry only:



The device combined lateral flow immunoassay with miniaturized paper electrodes for both colorimetric and electrochemical detection, providing a platform which can be further upgraded into wireless-enabled biosensing system in future.